JOURNAL OF GEOPHYSICAL RESEARCH, VOL. 107, NO. D21, 4583, doi:10.1029/2001JD001301, 2002

Relative source contribution analysis using an air trajectory statistical approach

Ching-Ho Lin
Department of Environmental Engineering and Sanitation, Fooyin Institute of Technology, Kaohsiung Hsien, Taiwan

Len-Fu W. Chang
Graduate Institute of Environmental Engineering, National Taiwan University, Taipei, Taiwan

Received 18 September 2001; revised 8 May 2002; accepted 20 June 2002; published 12 November 2002.

[1] An air trajectory statistical approach was developed to estimate the relative contributions of various sources within a planning domain for a receptor site during high air pollution. The proposed approach is based on the coupling of residence time analysis and a known emission inventory. The theoretical basis of the approach is detailed. The approach was applied to investigate the relative contributions of various anthropogenic volatile organic compound (VOC) sources to the ozone formation potential of a receptor site in southern Taiwan. One hundred and ninety-seven ozone events (defined as those with an hourly ozone concentration that exceeded 120 ppb standard) over 1994–1998 were selected to undergo the residence time analysis. The VOC emission inventory was adjusted to reflect the different ozone formation potentials of the various sources by considering the source VOC profiles and the maximum incremental reactivity scales of each VOC compound. The results show that the sources that influenced the evaluated receptor site were located in northwestern coastal regions; the relative contributions of the point, line, and area sources were in the ration of approximately 5:2:3. Two districts, Kaohsiung City and Kaohsiung Hsien, were the dominant contributors of the five investigated districts. The proposed method may act as a preliminary tool to efficiently select the potential source region/category, such that mitigation and control strategies can be targeted, and/or used to guide a comprehensive modeling study. *INDEX TERMS:* 0305 Atmospheric Composition and Structure: Aerosols and particles (0345, 4801); 0322 Atmospheric Composition and Structure: Constituent sources and sinks; 0345 Atmospheric Composition and Structure: Pollution—urban and regional (0305); 0365 Atmospheric Composition and Structure: Troposphere—composition and chemistry; *KEYWORDS:* relative source contribution function, ozone, back trajectories, source contributions, model, potential source contribution function

Citation: Lin, C.-H., and L.-F. W. Chang, Relative source contribution analysis using an air trajectory statistical approach, *J. Geophys. Res.*, *107*(D21), 4583, doi:10.1029/2001JD001301, 2002.

1. Introduction

[2] The analysis of source regions and their contributions to receptors is essential to the development of effective control strategies. Numerous air quality models have been developed, which can address the above issues [*Seinfeld and Pandis*, 1998; *National Research Council* (*NRC*), 1991; *Russell and Dennis*, 2000]. However, the considerable requirements for large sets of input data and computational resources make most existing air quality models highly sophisticated and, thus, difficult for general users to derive. These obstacles limit these models to case studies only. Challenges occasionally arise in selecting representative simulation cases [*Yu and Chang*, 2000; *NRC*, 1991; *Chang et al.*, 1987]. This work aims to develop a new approach to fill the gaps between the air quality models and simple trajectory analyses.

[3] Despite the extensive successes of current air quality models, many researchers choose the simple air trajectory analysis approach to identify the potential sources for specific receptors [*Cabezudo et al.*, 1997; *Chiapello et al.*, 1995, 1997; *Colin et al.*, 1989; *Stohl*, 1998]. That is, air trajectory analysis directly indicates the linkages between sources and receptors. For example, *Cabezudo et al.* [1997] confirmed the existence of pollen from northern Moroccan marihuana plantations in southern Spain; *Chiapello et al.* [1995, 1997] identified that the dust over the northeastern tropical Atlantic had originated from the Sahara and Sahel regions; *Colin et al.* [1989] determined that the compositions of species observed in rain and snow precipitation in eastern France were derived from several industrial sources.

[4] Moreover, the trajectory-based approach, as it pertains to air pollution, has been enhanced by the development of trajectory statistics. Originally, *Ashbaugh* [1983] and *Ash-*

0148-0227/02/2001JD001301

baugh et al. [1985] developed a trajectory statistical method to determine the locations of major pollutant sources, which affected a distant downwind receptor. This method is known as either residence time analysis (RTA) [*Poirot and Wishinski*, 1986; *Stohl*, 1996] or the potential source contribution function (PSCF) [*Zeng and Hopke*, 1989; *Cheng et al.*, 1993a, 1993b]. Notably, this approach traced back numerous air parcel trajectories with high pollutant concentrations to arrive at the receptor. The intersections among the trajectories were therefore deemed possible pollution sources.

[5] Many variations or theoretical analyses of the *Ashbaugh* [1983] method exist in the literature. For example, *Vasconcelos et al.* [1996a] used a bootstrapping technique and binomial distribution, to test the significance of PSCF and to reduce the statistical noise; *Cheng et al.* [1993b] presented an artificial factor to remove statistical noise. *Vasconcelos et al.* [1996b] explored spatial resolutions of the PSCF method and revealed that the method can resolve the direction of potential sources, but is less able to resolve their radial distances from the receptors. *Seibert et al.* [1994] weighted the residence time with a logarithmic mean concentration at the receptor sites and produced concentration fields to identify source areas of air pollutants. *Stohl* [1996] modified the Seibert et al. method to extract sources in hot spots more precisely than the usual ones. Variations of the Ashbaugh method have been applied to identify atmospheric aerosol sources for sulfate particulate [*Ashbaugh et al.*, 1985; *Poirot and Wishinski*, 1986; *Malm and Gebhart*, 1990; *Cheng et al.*, 1993a, 1993b; *Virkkula et al.*, 1995; *Stohl*, 1996], origin of ozone pollution [*Stohl and Kromp-Kolb*, 1994; *Sirois and Bottenheim*, 1995; *Dickerson et al.*, 1995; *Poirot and Wishinski*, 1998], sources of toxic air pollutants [*Gatz and Sweet*, 1998], and sources of chemical species in acid precipitation [*Barrie*, 1988; *Zeng and Hopke*, 1989]. Additionally, the PSCF method has been extended by *Gao et al.* [1993] and *Cheng et al.* [1996] to evaluate grid source contributions. These researchers used the PSCF value and timed the source emission in each grid to assess the grid source contributions for SOx and NOx, to the receptor sites of concern. *Stohl* [1998] reviewed more applications of air trajectory analyses.

[6] This paper further explores applications of air trajectory statistics in source contribution analysis. An air trajectory statistical approach is proposed to identify sources of influence, and evaluate their relative contributions to a receptor site of concern, during high air pollution. The present approach is similar to those developed by *Gao et al.* [1993] and *Cheng et al.* [1996]. However, the PSCF value used in those works was replaced with the probability of air parcel residence time. The following section details the theoretical basis and the assumptions of the new approach. The approach is then employed to evaluate the relative contributions of various anthropogenic VOC sources to the ozone formation potential of a receptor site in southern Taiwan, during ozone pollution.

2. Model Descriptions

[7] The following assumptions are made.

1. A rectangular planning area (an investigated domain) is considered for simplicity, and divided into $I \times J$ parts (grid cells).

2. S is the receptor site to be analyzed. The location of this site is prescribed and need not necessarily be within the investigated domain.

3. K air pollution events were observed at receptor site S, during the period considered.

4. The gridded emissions contained therein are known, but their relative contributions to the evaluated receptor pollution are unknown and are derived as follows.

[8] If $\Delta C(i, j, k)$ represents a concentration increment observed at receptor site S during the kth air pollution event, and this increment resulted from the source contribution in grid cell (i, j), then a statistically normalized contribution from grid cell (i, j) to the air pollution of the receptor site, S, can be expressed by a relative source contribution function (RSCF),

$$\mathrm{RSCF}(i,j) = \frac{\sum_{k=1}^{K} \Delta C(i,j,k)}{\sum_{i=1}^{I}\sum_{j=1}^{J}\sum_{k=1}^{K} \Delta C(i,j,k)}, \tag{1}$$

in which RSCF(i, j) is the RSCF value at the grid cell (i, j). RSCF(i, j) gives the total concentration increment contributed by grid cell (i, j) to all of the investigated domain through the K air pollution events. Obviously, the sum of RSCF over the entire domain is unity. The RSCF gives only the relative contributions for the sources in the investigated domain. The effects of the sources outside the domain, such as long-range transport, on the receptor pollution are unaccounted for. Therefore the domain should be selected to cover the major sources that influencing the receptor pollution.

[9] As mentioned earlier, air quality models can be applied to obtain the concentration increments in equation (1) and to provide the RSCF value. Models including detailed descriptions of emission patterns, meteorology, chemical transformation and removal processes, can be expected to yield a more reliable RSCF value. However, complicated models consistently require numerous input data sets and computational resources. Therefore analyzing large numbers of air pollution events with complicated models is impractical. Several assumptions are therefore made to estimate RSCF in the following sections.

[10] The pollutant concentrations observed at the receptor site, S, during the kth air pollution event, can be considered as the concentrations within a specific air parcel that has recently arrived at that site. Thus the concentration increment from the source contribution in grid cell (i, j) during the kth air pollution event can be expressed as

$$\begin{aligned}\Delta C(i,j,k) &= w(i,j,k) \times f(i,j,k) \\ &= \Delta t(i,j,k) \times e(i,j,k) \times f(i,j,k)\end{aligned} \tag{2}$$

in which $w(i, j, k)$ is the pollutant emission, which was swept into the air parcel during its journey within grid cell (i, j) in the kth air pollution event. The emission $w(i, j, k)$, can be calculated by the product of $\Delta t(i, j, k)$ and $e(i, j, k)$, which are the time for which the air parcel remained in grid cell (i, j) and the emission rate of grid cell (i, j), respectively, during the kth air pollution event. $f(i, j, k)$ is a pollutant transfer coefficient, which accounts for the

overall effects of atmospheric physical and chemical mechanisms while the air parcel travels from grid cell (i, j) to the receptor site at the kth air pollution event [*Keeler and Samson*, 1989]. Substituting equation (2), equation (1) becomes

$$\mathrm{RSCF}(i,j) = \frac{\sum_{k=1}^{K} \Delta t(i,j,k) \cdot e(i,j,k) \cdot f(i,j,k)}{\sum_{i=1}^{I}\sum_{j=1}^{J}\sum_{k=1}^{K} \Delta t(i,j,k) \cdot e(i,j,k) \cdot f(i,j,k)}. \quad (3)$$

[11] Two assumptions further simplify RSCF in equation (3). First, emission rates in all grid cells are assumed to be invariant with time:

$$e(i,j,k) = E_0(i,j), \quad (4)$$

in which $E_0(i, j)$ is the emission rate of grid cell (i, j), independent of all air pollution events. This assumption allows an average emission inventory, such as an annual one, to be directly applied.

[12] Second, all the pollutant transfer coefficients in equation (3), representing in various grid cells for various air pollution events, are assumed to be the same. This assumption allows the transfer coefficients in equation (3) to be eliminated and, therefore, simplifies the subsequent calculation. Notably, this assumption is more acceptable when the air parcels corresponding to all air pollution events experience similar transport patterns or when the pollutant is less reactive.

[13] With the above two assumptions, equation (3) can be reduced to

$$\mathrm{RSCF}(i,j) = \frac{RT(i,j) \cdot E_0(i,j)}{\sum_{i=1}^{I}\sum_{j=1}^{J} RT(i,j) \cdot E_0(i,j)}, \quad (5)$$

where $RT(i, j)$ is the residence time probability of grid cell (i, j) [*Ashbaugh*, 1983; *Ashbaugh et al.*, 1985], representing the period for which K air parcels remained in grid cell (i, j) to the period they spent in the whole investigated domain. $RT(i, j)$ can be estimated by calculating each back trajectory for each pollution event and counting the number of nodes along these K back trajectories that fall into each grid cell, since the intervals between the nodes are constant [*Ashbaugh et al.*, 1985; *Cheng et al.*, 1993a, 1993b; *Stohl*, 1996]. The residence time probability is then given by

$$RT(i,j) = \frac{\sum_{k=1}^{K} n(i,j,k)}{\sum_{i=1}^{I}\sum_{j=1}^{J}\sum_{k=1}^{K} n(i,j,k)}, \quad (6)$$

in which $n(i, j, k)$ represents the number of endpoints in grid cell (i, j) for the kth backward trajectory.

[14] Finally, equations (5) and (6) suggest the method for estimating RSCF. The value of RSCF in each grid cell can directly reveal the contribution of the grid cell to all the investigated sources. RSCF can be integrated over a specific subdomain, such as a district, to obtain the relative contribution of the subdomain sources. Moreover, once the gridded emission inventories can be divided into a lump of L categories, equation (5) can be extended to

$$\mathrm{RSCF}(i,j,l) = \frac{RT(i,j) \cdot E_0(i,j,l)}{\sum_{i=1}^{I}\sum_{j=1}^{J}\sum_{l=1}^{L} RT(i,j) \cdot E_0(i,j,l)}, \quad (7)$$

in which RSCF(i, j, l) and $E_0(i, j, l)$ are the relative source contribution and the source emission rate, respectively, for the lth category sources in grid cell, (i, j). Consequently, the relative contributions of the specific category sources in the subdomain can be obtained by integrating RSCF in equation (7) for specific category sources over a prescribed subdomain. The current approach can thus be used to estimate the relative contributions of the sources within a specific geophysical region, in a specific category, and in a specific combination of region and category. A feasible source combination would allow air quality mangers rapidly to evaluate the significance of different target sources.

3. Model Application

3.1. Problem Description

[15] Figure 1 shows the domain investigated here, which is located in south Taiwan. The computational domain is a fixed rectangle for simplicity. However, only five districts in this domain are considered. They are Tainan Hsien (TS), Tainan City (TC), Kaohsiung Hsien (KS), Kaohsiung City (KC), and Pingdong Hsien (PS). Accordingly, the emission rates outside the five districts are set to zero. The evaluated receptor site, located in the PS district, is an air quality monitoring station, namely Chao Zhou (CZ), which is maintained and operated by Taiwan's Environmental Protection Administration (EPA).

[16] The RSCF approach was followed to evaluate the relative contributions from various VOC sources within the domain, to the ozone formation potential at the CZ receptor site during high ozone pollution. The ozone pollution problem was serious at this site. As reported by Taiwan EPA, the CZ site violated the Taiwan EPA ozone 1-h standard of 120 ppb, for approximately 40 days per year during 1994–1998 [*Taiwan Environmental Protection Administration*, 1998].

3.2. Air Quality Data

[17] The Taiwan EPA air quality database of 1-h average ozone concentrations at the CZ station during 1994 to 1998 was examined to isolate the ozone pollution events for RSCF analysis. The ozone pollution events were defined as those days with a daily 1-hour maximum ozone concentration exceeding 120 ppb.

3.3. Trajectory Data

[18] The backward trajectories were calculated according to the hourly mixing-layer average wind fields on days of ozone pollution. The wind fields were determined according

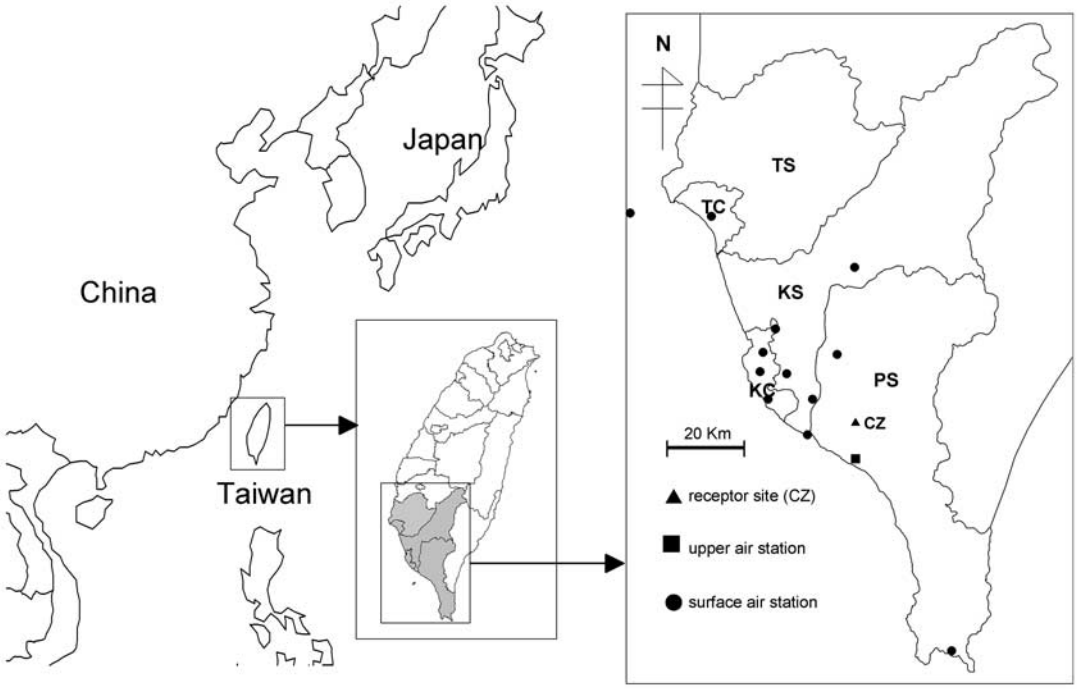

Figure 1. Investigated domain and meteorological stations.

to the method proposed by *Draxler* [1979]. This method used twice-daily rawinsonde data from upper air stations and hourly surface data from the much denser network of surface stations. Herein, data of one upper air station and 13 surface stations were used. Figure 1 shows the locations of these stations. Notably, other methods of trajectory calculation may be preferred over the method used here, since several improvements have been made to trajectory calculation since *Draxler* [1979] proposed his method, as reviewed by *Stohl* [1998]. For example, the trajectory calculation based on the wind fields produced from the numerical models could be expected to be superior to those based on the method used here. *Stohl and Wotawa* [1995] elucidated a useful method to calculate the trajectories of pollutant transport when the pollutants are released in the daytime, subsequently frozen in the residual layer aloft in the nighttime, and finally fumigated back to the ground in the following daytime.

[19] The backward trajectories were set to begin from the receptor site at the ozone peak time and end at either 02:00 or when the trajectories exited the computational domain on the selected ozone pollution days. The ozone typically peaked between 12:00 and 17:00. The end time of the backward trajectories was set to allow backward trajectory analysis over at least 12-hour period and to include rush-hour emission in the morning. The trajectory endpoints were recorded 12 times per hour. The endpoints in each 2 km by 2 km grid cell were counted to produce the residence time probability field according to equation (6). However, the final residence time probability field was smoothed with a 9-point weighting formula, to reduce statistical noise. The smoothing process was designed to redistribute the residence time probability in each initial calculated grid cell over a 3 by 3 grid cell array, centered on the considered grid cell, according to the inverse of the distance from the array center to the redistributed grid cells, that is,

$$\begin{aligned} RT_{new}(i,j) = {} & RT_{old}(i,j) \times 3/15 + RT_{old}(i+1,j) \times 2/15 \\ & + RT_{old}(i-1,j) \times 2/15 + RT_{old}(i,j+1) \times 2/15 \\ & + RT_{old}(i,j-1) \times 2/15 + RT_{old}(i+1,j+1) \times 1/15 \\ & + RT_{old}(i-1,j+1) \times 1/15 + RT_{old}(i+1,j-1) \times 1/15 \\ & + RT_{old}(i-1,j-1) \times 1/15, \end{aligned} \tag{8}$$

in which $RT(i, j)$ is the residence time probability of grid cell (i, j), and the subscripts *new* and *old* correspond to after and before the smoothing process, respectively.

3.4. Emission Data

[20] The VOC emission data in the five districts of interest was extracted from the newest version of Taiwan Emission Data System (TEDs 4.2) [*Taiwan Environmental Protection Administration*, 1999]. The TEDs emission database, developed in 1991 by the Taiwan EPA, includes source emissions throughout Taiwan. TEDs 4.2 is an updated version, based on 1997 source activity. The main source categories in TEDs are point, line and area. Point sources are generally stationary and large emitters. Line sources are the road vehicles. Area sources are fugitives and small emitters. The TEDs emission database also provides emissions in detailed source categories, based on manufacturing processes and vehicle types. The emissions for each source in a detailed category were first divided into various VOC species according to the profiles in the SPECIATE database, version 1.5 [*U.S. Environmental Protection Agency*, 1992] to account for the different ozone formation potentials from various sources. Second, the VOC species

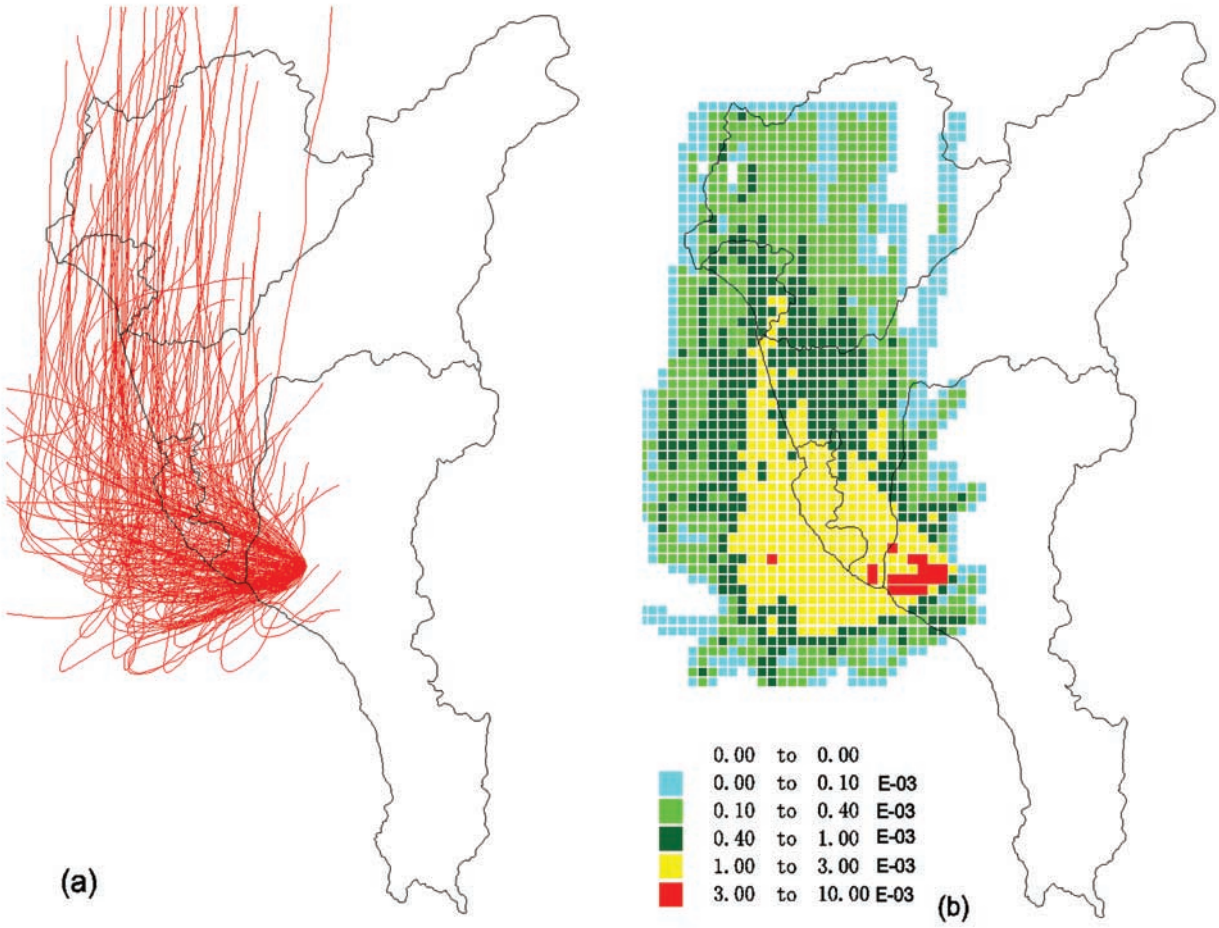

Figure 2. (a) Backward trajectories arriving at the CZ receptor site on days of ozone pollution in 1994–1998. (b) Residence time probability from 2 km × 2 km grid cells.

emissions were weighted by their corresponding MIR scales [*Carter*, 1994]. The MIR scales developed by Carter were calculated from the effects of VOC species on ozone formation potential [*Carter*, 1994, 1995; *Carter et al.*, 1995]. Finally, the weighted VOC species emissions for each detailed category source were summed to a MIR-weighted VOC emission. Subsequently, the gridded emission inventories of the main source categories (point, line and area) were prepared by accumulating the MIR-weighted VOC emissions for sources within each 2 km × 2 km grid cell. These MIR-weighted VOC gridded emission inventories were, therefore, used to determine the relative source contributions to the ozone formation potential at the CZ receptor sites during ozone pollution.

4. Results and Discussion

[21] A total of 197 ozone pollution events were selected. Figure 2a shows the corresponding backward trajectories of these events. Numerous trajectories were terminated within the investigated domain, since they normally ended at 02:00 on the selected ozone pollution days. *MacKenzie et al.* [1995] observed a major peak in the plume ozone increment 6–8h downwind of post rush-hour release in urban centers. The current termination time was therefore sufficient to gauge the effects of "one day episodes." Figure 2a also shows that trajectories were mostly derived from the northwest part of the receptor, and only seldom from the eastern part. Most trajectories experienced a major direction change before arriving at the receptor site. These trajectory patterns agreed with the weather presented by *Yu and Chang* [2000], who found that a general ozone event in southern Taiwan typically relates to a weak northerly wind at night and a weak westerly sea breeze during the following day.

[22] Figure 2b shows the residence time probability map, calculated from the backward trajectories of the 197 ozone pollution events. Only sources within grid cells with a residence time probability exceeding zero (not blank cells) can contribute to ozone formation potential at the receptor site CZ. Accordingly, as shown in Figure 2b, potential influencing sources are located in the northwest quarter of the receptor site.

[23] The grid cells with a residence time probability at the first level, 3.00×10^{-3}–10.00×10^{-3}, mark out a small area just to the west of the receptor site (Figure 2b). As all trajectories converge from the west to the receptor site (Figure 2a). The area with the second highest residence time probability, $1.00 \times 10^{-3} - 3.00 \times 10^{-3}$, extends outward from the first level region in both northwest and southwest directions and depicts a triangular region. Gen-

Table 1. MIR-Weighted VOC Emissions for Point, Line, and Area Sources in Various Districts in South Taiwan

	MIR-Weighted VOC Emission Rate							
	Point Sources		Line Source		Area Sources		Total	
District	Tons per Day	Percent	Tons per Day	Percent	Tons per Day	Percent	Tons per Day	Percent
KC	161	10.9	131	8.8	108	7.3	401	26.9
TC	1	0.1	69	4.6	43	2.9	113	7.6
TS	53	3.6	79	5.3	114	7.6	245	16.5
KS	350	23.5	82	5.5	167	11.2	599	40.3
PS	3	0.2	60	4.0	67	4.5	130	8.8
Total	568	38.2	421	28.2	499	33.5	1488	100.0

erally, the residence time probability decreases in the northwestern and southwestern directions, as the distance from the receptor site increases. Integrating the grid cell probability over each individual district region, reveals that the accumulated probabilities of the fives districts are KS (19%) > PS (15%) > TS (9%) > KC (8%) and TC (3%), respectively. 47% of the probability fell outside the five districts. Most of the probability was in the sea area (Figure 2b).

[24] In 1997, the MIR-weighted VOC emission for anthropogenic sources in south Taiwan was about 1500 ton day^{-1} (Table 1). Figures 3a–3d show the gridded emissions for point, line, and area sources, and the total, respectively. Most point sources are distributed near the west coastal region and cover a band from the south of KS district to the north of TS district (Figure 3a). Major line sources are observed in the KC and TC districts due to the intensive population and high road density in these two cities (Figure 3b). Figure 3b also depicts the locations of several significant highways. The area sources (Figure 3c) are distributed over the entire investigated domain. However, major sources are also found in the west coastal region.

[25] The ranks and the MIR-weighted VOC emission contribution levels for the three source categories (Table 1) are point (38%) > area (34%) > line (28%). Those for the five districts are KS (40%) > KC (27%) > TS (17%) > PS (9%) > TC (8%), respectively. The above rankings and contribution levels, in source categories or districts, differ significantly from those obtained by RSCF analyses.

[26] Figures 4a–4d show the relative contributions to the ozone formation potential at the CZ station of point, line, area sources, and the total, over southern Taiwan on dates with ozone pollution, determined by RSCF analysis. The region covering the east and south of the receptor site is blank in Figures 4a–4d, implying that no sources within this blank region contributed to the ozone formation potential of the receptor site. In contrast, sources in the northwest quarter of the receptor site dominated. No difference between the spatial distribution patterns of the point source emission map (Figure 3a) and those of the point source RSCF map (Figure 4a) is apparent, because most point sources in southern Taiwan are practically located within the region that the air parcels passed, as observed in Figures 2 and 3a. However, the RSCF analysis (Figure 4a) indicated that three grid cells with large emission rates located in the TS district (Figure 3a) significantly lost their contribution levels, due to a smaller residence time probability in that district (Figure 2b). The difference between the line source emission map (Figure 3b) and RSCF map (Figure 4b) is evident. As mentioned above, RSCF analysis showed that area sources in the east and south of the receptor completely ceased to contribute (Figure 4c). Only the area source at the northwest coastal region of the receptor site dominated the contributions.

[27] Table 2 lists the relative contributions for point, line and area sources in the five districts, determined by RSCF analysis. The table reveals that the ranking order and contribution levels of the three source categories are point (49%) > area (29%) > line (22%). The contribution levels of the three category sources differ significantly from those based on the VOC emission levels (Table 1). The point sources exhibit a 10% increase in the RSCF-based contribution levels than the emission-based. In contrast, area and line sources exhibit 6% and 4% decreases, respectively. The contribution level variations of the three category sources resulted from the spatial distributions of the residence time probability and source spatial distributions. As mentioned above, most point sources in southern Taiwan are located within the region that the air parcels passed. Therefore point sources have higher air parcel retention times than line and area sources. As a result, the contribution of point sources increase and those of line and area sources decrease.

[28] The ranking and the contribution levels of the five districts determined by RSCF analysis are KS (49%) > KC (37%) > PS (5.5%) > TC (4.6%) > TS (4.3%) (Table 2). These contribution levels in each district change significantly from those based on the VOC emission levels (Table 1). KC and KS districts show 10% and 9% increases, respectively, in their contributions. However, the contribution levels of TS, PS and TC districts decline greatly. In summary, the dominant contributors to the ozone formation potential at the CZ station on days of ozone pollution were the KS and KC districts. The districts together accounted for 86% of the total relative contributions. Considering specific combinations of source categories and districts, KS point sources (32%), KC point sources (15%), KS area sources (13%), KC line sources (12%) and KC area sources (10%) totally contributed 82% of the total relative contribution, and were thus the main contributors.

5. Conclusion

[29] An air trajectory statistical approach, namely RSCF analysis, was developed to investigate the relative source contributions to a receptor site of concerned. The presented approach was therefore used to evaluate ozone formation potential at a receptor site, from various anthropogenic VOC sources in southern Taiwan on days of ozone pollution. MIR-weighted VOC emission rates were used in the

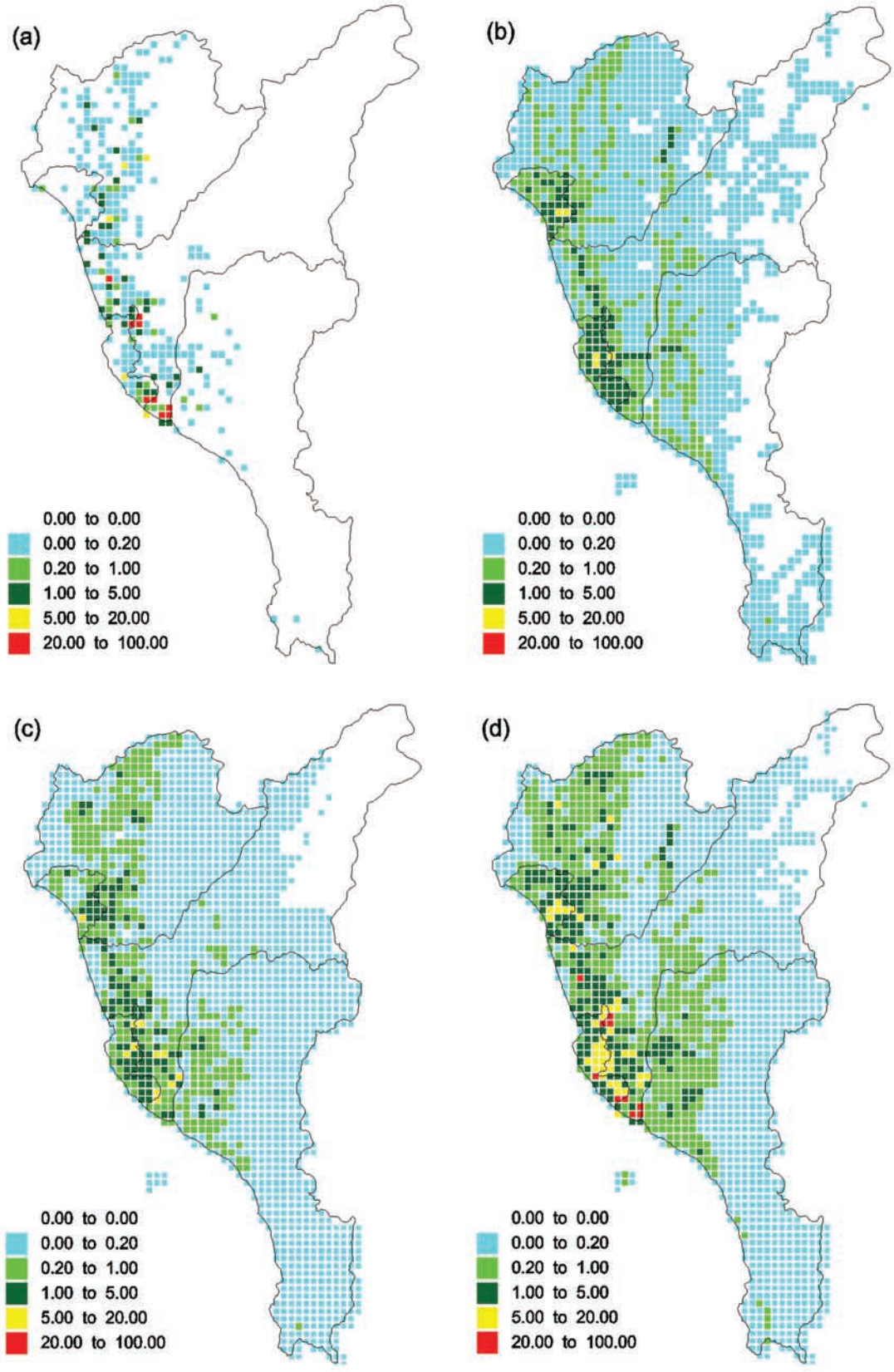

Figure 3. MIR-weighted VOC emission (ton day^{-1}) from 2 km $\times$ 2 km grid cells for (a) point, (b) line, (c) area, and (d) all sources, in south Taiwan.

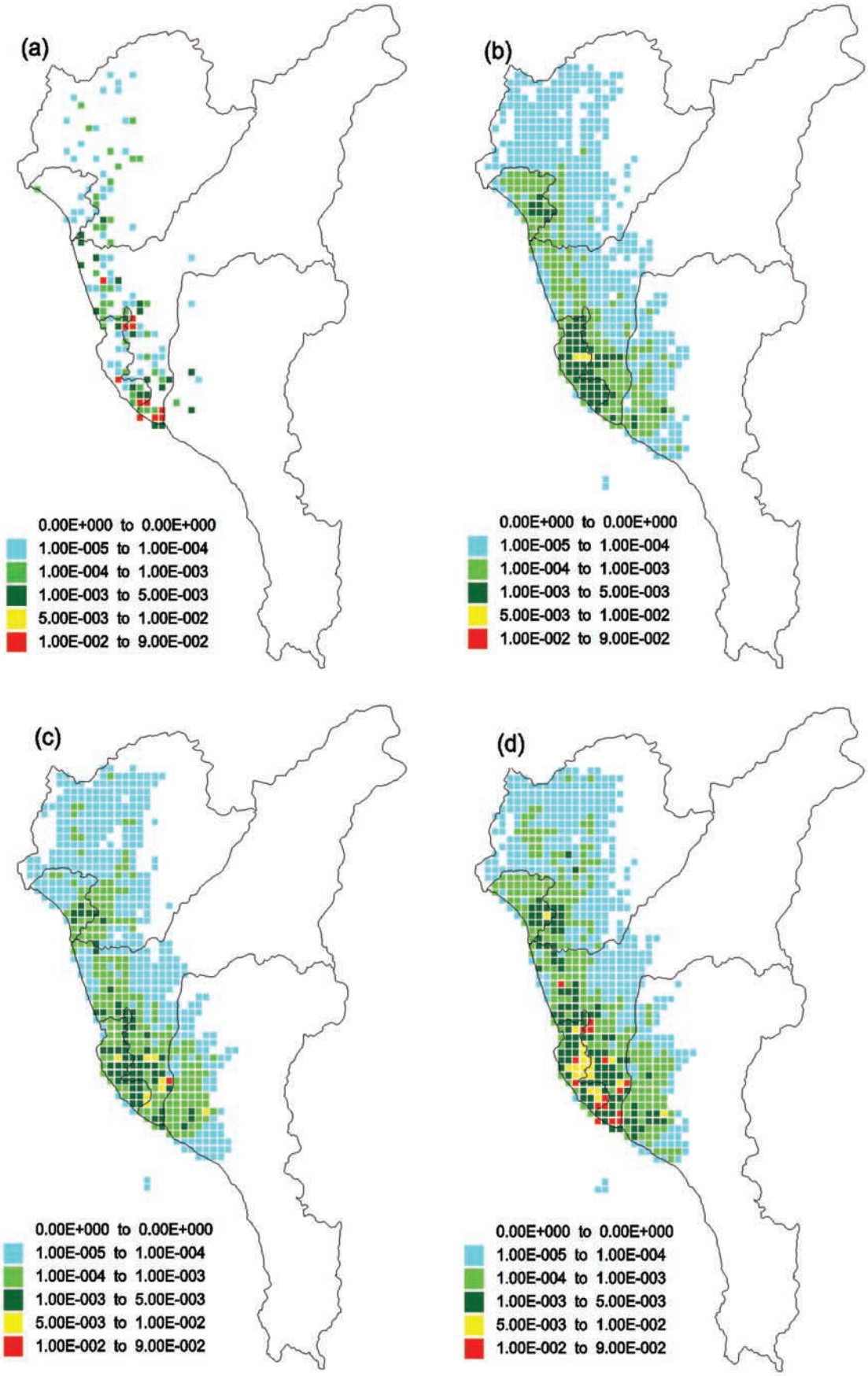

Figure 4. RSCF maps for (a) point, (b) line, (c) area, and (d) all sources.

Table 2. Relative Contributions to the Ozone Formation Potential at the CZ Station of Various Source Categories and Districts in South Taiwan, Determined by RSCF Analysis

	Contribution, %			
District	Point Sources	Line Sources	Area Sources	Total
KC	15.0	12.0	9.5	36.5
TC	<0.1	2.8	1.8	4.6
TS	1.4	1.0	2.0	4.3
KS	32.0	4.3	12.7	49.0
PS	0.3	2.0	3.3	5.5
Total	48.7	22.0	29.3	100.0

RSCF analyses to accommodate different reactivity scales of various VOC sources. The results show that the sources that affected the evaluated receptor site were located in the northwestern coastal regions. The relative contributions of the point, line and area category sources were approximately 5:2:3. KC and KS were the dominant contributors of the five investigated districts. The major contributors, in terms of specific combinations of source categories and districts, were KS point sources, KC point sources, KS area sources, KC line sources and KC area sources. These major contribution sources could be arranged in the first priority for the development of source reduction strategies or for deeper modeling analysis.

[30] The current approach extends the application of trajectory statistics and provides a tool for simply estimating the relative significance of various investigated sources to pollution at the receptor. However, the effects of the differences of atmospheric dispersion, chemical transformation and/or depositions in each case analysis are not considered here. Further work should address this omission. The strengths of this approach rely on the analysis of larger numbers of air pollution events, the limits of correctly calculated back trajectories, and the uncertainties of the emission inventory used.

[31] **Acknowledgments.** The authors would like to thank the National Science Council, Taiwan, for financially supporting this research under contract NSC 89-2211-E-242-007.

References

Ashbaugh, L. L., A statistical trajectory technique for determining air pollution source regions, *J. Air Pollut. Control Assoc.*, *33*, 1096–1098, 1983.

Ashbaugh, L. L., W. C. Malm, and W. Z. Sadeh, A residence time probability analysis of sulfur concentrations at Grand Canyon National Park, *Atmos. Environ.*, *19*, 1263–1270, 1985.

Barrie, L. A., Aspects of atmospheric pollutant origin and deposition revealed by multielemental observations at a rural location in eastern Canada, *J. Geophys. Res.*, *93*, 3773–3788, 1988.

Cabezudo, B., M. Recio, J. M. Sanchez-Laulhe, M. D. M. Trigo, F. J. Toro, and F. Polvorinos, Atmospheric transport of marihuana pollen from North Africa to the southwest of Europe, *Atmos. Environ.*, *31*, 3323–3328, 1997.

Carter, W. P. L., Development of ozone reactivity scales for volatile organic compounds, *J. Air Waste Manage. Assoc.*, *44*, 881–889, 1994.

Carter, W. P. L., Computer modeling of environmental chamber measurements of maximum incremental reactivities, *Atmos. Environ.*, *29*, 2513–2527, 1995.

Carter, W. P. L., J. A. Pierce, D. Luo, and I. L. Malkina, Environmental chamber study of maximum incremental reactivities of organic compounds, *Atmos. Environ.*, *29*, 2499–2511, 1995.

Chang, J. S., R. A. Brost, I. S. A. Isaksen, S. Madronic, P. Middleton, W. R. Stockwell, and C. J. Walcek, A three-dimensional Eulerian acid deposition model: Physical concepts and formulation, *J. Geophys. Res.*, *92*, 14,681–14,700, 1987.

Cheng, M.-D., P. K. Hopke, L. Barrie, A. Rippe, M. Olson, and S. Landsberger, Qualitative determination of source regions of aerosol in Canadian high Arctic, *Environ. Sci. Technol.*, *27*, 2063–2071, 1993a.

Cheng, M.-D., P. K. Hopke, and Y. Zeng, A receptor-oriented methodology for determining source regions of particulate sulfate observed at Dorset, Ontario, *J. Geophys. Res.*, *98*, 16,839–16,849, 1993b.

Cheng, M. D., N. Gao, and P. K. Hopke, Source apportionment study of nitrogen species measured in southern California in 1987, *J. Environ. Eng.*, *122*, 183–190, 1996.

Chiapello, I., G. Bergametti, L. Gomes, B. Chatenet, F. Dulac, J. Pimenta, and E. S. Suares, An additional low layer transport of Sahelian and Saharan dust over the North-Eastern Tropical Atlantic, *Geophys. Res. Lett.*, *22*, 3191–3194, 1995.

Chiapello, I., G. Bergametti, B. Chatenet, P. Bousquet, F. Dulac, and E. S. Soares, Origins of African dust transport over the northeastern tropical Atlantic, *J. Geophys. Res.*, *102*, 13,701–13,709, 1997.

Colin, J. L., D. Renard, V. Lescoat, and J. L. Jaffrezo, Relationship between rain and snow acidity and air mass trajectory in eastern France, *Atmos. Environ.*, *23*, 1487–1498, 1989.

Dickerson, R. R., B. G. Doddridge, and P. Kelley, Large-scale pollution of the atmosphere over the remote Atlantic Ocean: Evidence from Bermuda, *J. Geophys. Res.*, *100*, 8945–8952, 1995.

Draxler, R. R., Modeling the results of two recent mesoscale dispersion experiments, *Atmos. Environ.*, *13*, 1523–1533, 1979.

Gao, N., M.-D. Cheng, and P. K. Hopke, Potential source contribution function analysis and source apportionment of sulfur species measured at Rubidoux, CA during the Southern California Air Quality Study, 1987, *Anal. Chim. Acta*, *277*, 369–380, 1993.

Gatz, D. F., and C. W. Sweet, Source identification of Great Lakes toxic air pollutants, 98-RA89.01, paper presented at 91st Air and Water Management Association Annual Meeting and Exhibition, San Diego, Calif., 14–18 June, 1998.

Keeler, G. J., and P. J. Samson, Spatial representativeness of trace element ratios, *Environ. Sci. Technol.*, *23*, 1358–1364, 1989.

MacKenzie, A. R., R. M. Harrison, I. Colbeck, P. A. Clark, and R. H. Varey, The ozone increments in urban plumes, *Sci. Total Environ.*, *159*, 91–99, 1995.

Malm, W. C., and K. A. Gebhart, An investigation of the dominant source regions of fine sulfur in the western United States and their areas of influence, *Atmos. Environ., Part A*, *24*, 3047–3060, 1990.

National Research Council, *Rethinking the Ozone Problem in Urban and Regional Air Pollution*, Nat. Acad., Washington, D. C., 1991.

Poirot, R. L., and P. R. Wishinski, Visibility, sulfate and air mass history associated with the summertime aerosol in northern Vermont, *Atmos. Environ.*, *20*, 1457–1469, 1986.

Poirot, R. L., and P. R. Wishinski, Long-term ozone trajectory climatology for the eastern US, 2, Results, 98-TP43.06 (A615), paper presented at the 91st Air and Water Management Association Annual Meeting and Exhibition, San Diego, Calif., 14–18 June, 1998.

Russell, A., and R. Dennis, NARSTO critical review of photochemical models and modeling, *Atmos. Environ.*, *34*, 2283–2324, 2000.

Seibert, P., H. Kromp-Kolb, U. Baltensperger, D. T. Jost, and M. Schwikowski, Trajectory analysis of high alpine air pollution data, in *Air Pollution Modelling and Its Application*, vol. 5, edited by S. E. Gryning, M. M. and Millan, pp. 595–596, Plenum, New York, 1994.

Seinfeld, J. H., and S. N. Pandis, *Atmospheric Chemistry and Physics*, John Wiley, New York, 1998.

Sirois, A., and J. W. Bottenheim, Use of backward trajectories to interpret the 5-year record of PAN and O_3 ambient air concentrations at Kejimkujik National Park, Nova Scotia, *J. Geophys. Res.*, *100*, 2867–2881, 1995.

Stohl, A., Trajectory statistics—A new method to establish source-receptor relationships of air pollutants and its application to the transport of particulate sulfate in Europe, *Atmos. Environ.*, *30*, 579–587, 1996.

Stohl, A., Computation, accuracy and applications of trajectories—A review and bibliography, *Atmos. Environ.*, *32*, 947–966, 1998.

Stohl, A., and H. Kromp-Kolb, Origin of ozone in Vienna and surroundings, Austria, *Atmos. Environ.*, *28*, 1255–1266, 1994.

Stohl, A., and G. Wotawa, A method for computing single trajectories representing boundary layer transport, *Atmos. Environ.*, *29*, 3235–3238, 1995.

Taiwan Environmental Protection Administration, *Air Pollution Control Review Reports*, Taipei, Taiwan, 1998.

Taiwan Environmental Protection Administration, *Taiwan Emission Data Systems Versions 4.2*, Taipei, Taiwan, 1999.

U.S. Environmental Protection Agency, *VOC/PM Speciation Data System, Version 1.5*, Research Triangle Park, N. C., 1992.

Vasconcelos, L. A. P., J. D. W. Kahl, D. Liu, E. S. Macias, and W. H.

White, A tracer calibration of back trajectory analysis at the Grand Canyon, *J. Geophys. Res.*, *101*, 19,329–19,335, 1996a.

Vasconcelos, L. A. P., J. D. W. Kahl, D. Liu, E. S. Macias, and W. H. White, Spatial resolution of a transport inversion technique, *J. Geophys. Res.*, *101*, 19,337–19,342, 1996b.

Virkkula, A., M. Makinen, R. Hillamo, and A. Stohl, Atmospheric aerosol in the Finnish Arctic: Particle number concentrations, chemical characteristics, and source analysis, *Water Air Soil Pollut.*, *85*, 1997–2002, 1995.

Yu, T. Y., and L. F. W. Chang, Selection of the scenarios of ozone pollution at southern Taiwan area utilizing principal component analysis, *Atmos. Environ.*, *34*, 4499–4509, 2000.

Zeng, Y., and P. K. Hopke, A study of the sources of acid precipitation in Ontario, Canada, *Atmos. Environ.*, *23*, 1499–1509, 1989.

L.-F. W. Chang, Graduate Institute of Environmental Engineering, National Taiwan University, 71 Chou-Shan Road, Taipei 106, Taiwan. (lfwchang@ms.cc.ntu.edu.tw)

C.-H. Lin, Department of Environmental Engineering and Sanitation, Fooyin Institute of Technology, 151 Ching-Hsuen Road, Ta-Liao Hsiang, Kaohsiung Hsien 831, Taiwan. (chlin@mail.fy.edu.tw)